



A STUDY ON THE INTERRELATION OF SEISMIC INTENSITY PARAMETERS AND DAMAGE INDICES OF STRUCTURES UNDER MAINSHOCK-AFTERSHOCK SEISMIC SEQUENCES

A. Elenas⁽¹⁾, I.M. Siouris⁽²⁾, A. Plexidas⁽³⁾

⁽¹⁾ Professor, Democritus Univ. of Thrace, Department of Civil Engineering, GR-67100 Xanthi, Greece
Email: elenas@civil.duth.gr

⁽²⁾ Senior researcher, Democritus Univ. of Thrace, Department of Civil Engineering, GR-67100 Xanthi, Greece
Email: jsiou@pme.duth.gr

⁽³⁾ Junior researcher, Democritus Univ. of Thrace, Department of Civil Engineering, GR-67100 Xanthi, Greece
Email: aplexida@civil.duth.gr

Abstract

The interrelation between seismic intensity parameters and the postseismic damage state of structures is investigated, with respect to mainshock-aftershock sequence-type ground motions. Several peak, energy, and spectral intensity parameters are implemented to describe the seismic damage potential. Overall structural damage indices (OSDIs) are used to designate the postseismic damage status of buildings. The interrelation between the seismic intensity parameters and the OSDIs is quantified by the Pearson correlation coefficient and by the Spearman rank correlation coefficient. The proposed procedure has been applied to a reinforced concrete structure. Following the design procedure, nonlinear dynamic analyzes are conducted to deliver the seismic structural response. The present investigation utilizes 75 natural accelerograms, recorded worldwide in regions with strong seismic activity. All the records are mainshock-aftershock seismic sequences. The numerical results show that the examined damage indices exhibit strong interrelation and the same degree of correlation to the examined seismic parameters. Analytical examination shows that both, the energy and the spectral seismic intensity parameters have the strongest correlation with the OSDIs while the peak seismic intensity parameters and the strong motion duration defined by Trifunac and Brady exhibit poor correlation with the OSDIs.

Keywords: Seismic Parameters, Damage Indices, Seismic Aftershocks, Reinforced Concrete, Correlation Study

1. Introduction

Earthquakes are usually part of a sequence of ground motions which can be defined as foreshocks, mainshocks, and aftershocks. Most aftershocks are located over the full area of fault rupture, and either occurs along the fault plane itself or other faults within the volume affected by the strain associated with the mainshock. Strong aftershocks can cause extensive structural damage due to their enormous intrinsic energy. As the magnitude of the mainshock increases, so does the number, magnitude and time span of the aftershocks that occur over time.

The original investigation about the seismic sequence can be traced to the end of 19th century, which is conducted by Omori in 1894 [1]. In his work, Omori concluded that the rate of aftershocks decayed inversely with time after the mainshock. After the Omori's work, many researchers investigated the nature of seismic sequence, and abundant knowledge was obtained in the field of seismology. There have been several investigations aimed at studying the effect of seismic sequences on the response of civil engineering structures. Some of them have been focused on the nonlinear response of single-degree-of-freedom (SDOF) systems while others in the response of multiple-degree-of-freedom (MDOF) systems. Regarding the effects of mainshock-aftershock sequence-type ground motions on structures, Mahin showed that strong aftershocks in the Managua earthquake sequence may double the displacement ductility demands of many elastoplastic single-degree-of-freedom (SDOF) systems [2, 3]. Further, Ruiz-García et al. [4] examined the response of 9 typical low-height reinforced concrete highway bridges under 26 as-recorded (natural ground motion recordings) mainshock-



aftershocks sequences gathered in the subduction zone of the Mexican Pacific Coast. They found that aftershocks did not significantly increase drift demands due to the inherent overstrength in their case-study on low-height highway bridges. Using incremental dynamic analysis, they showed that the effect of aftershocks tends to increase both peak and residual drift demands when the bridge models behave nonlinearly during the mainshock. According to them, the increment in drift demands depends on the level of the ground motion's intensity and the type of hysteretic behavior applied to the bridge columns. Hatzigeorgiou and Liolios [5] studied the response of 4 regular and 4 irregular reinforced concrete frames under 5 natural and 40 artificial seismic sequences. They concluded that multiple earthquakes required increased ductility and displacement demands in comparison with single seismic events. Furthermore, the seismic damage for multiple earthquakes is higher than that for single ground motions and as a result of the traditional seismic design procedures, which are essentially based on the isolated 'design earthquake', should be reconsidered since the multiple earthquakes phenomenon cannot be overlooked. Moreover, they highlighted the fact that sequential ground motions strongly affect the development and distribution of plastic hinges, which can be different from that for the case of single/isolated seismic events. Also, Ruiz-García and Negrete-Manriquez [6] studied the effect of aftershocks in steel framed buildings. For that reason, they made use of three steel moment-resisting frames and subjected them to a set of mainshock-aftershock seismic sequences. From the results of this investigation, unlike previous results based on artificial seismic sequences, it was found that the recorded aftershocks do not significantly increase peak and residual drift demands since the predominant period of the aftershocks is very different from the fundamental period of the frame models. Also, it was shown that artificial seismic sequences could significantly overestimate median peak and residual drift demands as well as the record-to-record variability. Their proposal was that the effect of aftershocks should be taken into account with the use of real mainshock-aftershock seismic sequences instead of artificial sequences, as well as site-specific seismic scenarios due to the particular dependency on ground motion features. Conclusively, we can infer that a structure already damaged from a mainshock and not yet repaired, may be incapable of resisting the excitation of the strong aftershocks, causing either become completely unusable or collapsed. This significant characteristic indicates that the influence of seismic sequences cannot be ignored [7].

The results of earthquakes pose a serious scientific and social problem because strong ground motions can cause enormous damage to infrastructure which can lead to serious injuries and death. Usually, a large mainshock is followed by numerous aftershocks some of them of significant intensity and duration, deteriorating the structural state of already damaged buildings. As a result, the danger of collapse increases after every aftershock if the time span between two consequential strong ground motions is not sufficient for the necessary repairs to be made. The degradation of stiffness and strength of a structure through the seismic sequence can be evaluated with the use of specific damage indicators. The assessment of danger from the ongoing seismic activity requires tools capable of instantly predicting the level of seismic threat that a strong aftershock poses to a structure. For that reason, the evaluation of seismic threat through the use of certain seismic parameters which present a high correlation level with the structural condition of many buildings becomes a powerful tool for the authorities to assess the seismic danger. Postseismic field observations and numerical investigations have indicated the interdependency between the seismic parameters and the damage status of buildings after earthquakes [8, 9, 10, and 11]. It can be safely inferred from past studies that the higher the destructive potential of an earthquake, the higher the amount of energy that structures are subjected to, increasing the probability of occurring greater damages and more rapid degradation of its stiffness and load bearing capability. In this work, several seismic parameters have been chosen in search of those who present a high interdependency level with certain seismic indices. Regarding simulating the mainshock-aftershock sequence, two natural accelerograms recorded from the same station in a short period have been combined to create an artificial accelerogram that simulates the seismic sequence in a particular area of interest. The used seismic records are provided by the databases of the Greek Institute of Engineering Seismology and Earthquake Engineering (ITSAK), the European Strong-Motion Data (ESD), the U.S. Geological Survey (USGS), the National Research Institute for Earth Science and Disaster Prevention (NIED) in Japan, the GeoNet Data Center (GEONET) in New Zealand and the General Directorate of Disaster Affairs (GDDA) in Turkey. The new artificial accelerograms were used as input files to conduct nonlinear dynamic analysis with the use of IDARC 2D [12], to furnish the OSDIs. Finally, a correlation study shows the interrelation between the examined seismic intensity parameters and the OSDIs.



2. Seismic Intensity Parameters

Seismic intensity parameters that represent the destructive potential of a seismic excitation can be identified after the event. Extracting ground motion parameters help track structural damage, as well as architectural condition and equipment integrity, thus determining the parameters of the dynamic behavior of structures of paramount importance.

In this study, 39 intensity parameters are utilized. The particular set used, tends to approach the interrelationship with the selected overall damage indices from multiple aspects. These parameters can be classified into three key categories namely: peak, spectral and energy. The chosen set encompasses the following: peak ground acceleration (PGA); peak ground velocity (PGV); peak ground displacement (PGD); the ratio PGA/PGV; Arias intensity (I_0); root mean square acceleration (RMS_a); strong motion duration as defined by Trifunac/Brady ($SMD_{T/B}$), by Donovan SMD (SMD_{Don}), by Trifunac/Novikova SMD ($SMD_{T/N}$) and by McCann SMD (SMD_{McCann}); 0.05g bracketed SMD ($SMD_{B0.05}$), 0.10g bracketed SMD ($SMD_{B0.10}$), seismic power based on the SMD of Trifunac/Brady ($P_{0.90}$), on the 0.05g bracketed SMD ($P_{B0.05}$), on the 0.10g bracketed SMD ($P_{B0.10}$), on the Donovan SMD (P_{Don}), on the Trifunac/Novikova SMD ($P_{T/N}$) and on the McCann SMD (P_{McCann}); spectral intensities of Housner (SI_H), of Kappos (SI_K), of Martinez-Rueda (SI_{MR}), of Hidalgo/Clough ($SI_{H/C}$), of Nau/Hall ($SI_{N/H}$), of Matsumura (SI_M), of modified Matsumura (SI_{Mmod}); effective peak acceleration (EPA); maximum effective peak acceleration (EPA_{max}); seismic energy input (E_{inp}); cumulative absolute velocity (CAV); cumulative absolute displacement (CAD); cumulative area under the absolute displacement time history (CAX); the seismic damage potential of Araya/Saragoni ($DP_{A/S}$); central period (CP); ratio 1/CP (1/CP); spectral acceleration (SA); spectral velocity (SV); spectral displacement (SD); the intensity of Fajfar/Vidic/Fischinger ($I_{F/V/F}$); and earthquake type after Meskouris (T_M). Table 1 shows a synoptic list of the used parameters and the corresponding references, where their definitions are provided. All the above-mentioned seismic intensity parameters have been evaluated for all the utilized acceleration time histories (both mainshock and mainshock-aftershock seismic sequences) by a computer-supported analysis.

Table 1 – Seismic Parameters.

Number	Seismic parameters	Reference	Number	Seismic parameters	Reference
1	PGA	[13]	21	$SMD_{T/B}$	[23]
2	PGV	[13]	22	$SMD_{B0.05}$	[24]
3	PGD	[13]	23	$SMD_{B0.10}$	[24]
4	PGA/PGV	[13]	24	SMD_{Don}	[25]
5	CP	[14]	25	$SMD_{T/N}$	[26]
6	1/CP	[14]	26	SMD_{McCann}	[27]
7	SI_H	[15]	27	$P_{0.90}$	[28]
8	SI_K	[16]	28	$P_{B0.05}$	[28]
9	SI_{MR}	[17]	29	$P_{B0.10}$	[28]
10	$SI_{H/C}$	[18]	30	P_{Don}	[28]
11	$SI_{N/H}$	[19]	31	$P_{T/N}$	[28]
12	T_M	[20]	32	P_{McCann}	[28]
13	EPA	[21]	33	$I_{F/V/F}$	[29]
14	EPA_{max}	[21]	34	E_{inp}	[30]
15	CAV	[8]	35	SI_M	[31]
16	CAD	[8]	36	SI_{Mmod}	[31]
17	CAX	[8]	37	$DP_{A/S}$	[32]
18	SD	[22]	38	I_0	[33]
19	SV	[22]	39	RMS_a	[13]
20	SA	[22]			

3. Seismic Acceleration Time Histories

According to the methodology, the expected damage potential of a seismic excitation on a structure is the main reason in selecting of the accelerograms. A set of globally occurred natural earthquakes has been utilized in this study. The selected seismic excitations cover all possible degrees of damage i.e. from low to severe. The present investigation utilized 75 worldwide acceleration records, created from two natural accelerograms of substantial seismic power, which were collected in the same area and a short time-gap between the two recordings. Table 2, indicates the data of all used seismic events. Figure 1, presents the creation of an artificial accelerogram from two natural recordings that represent the mainshock-aftershock sequence.

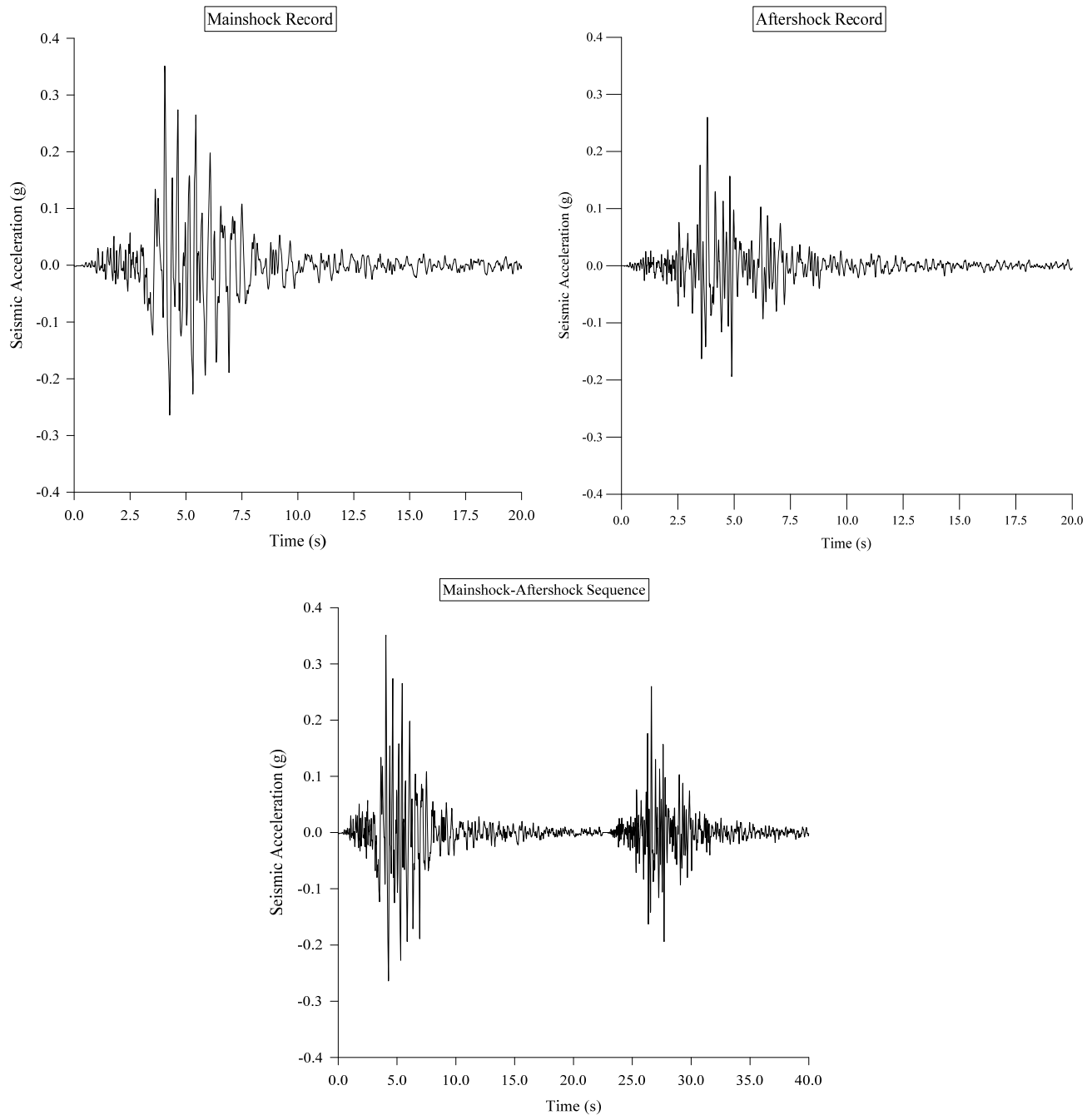


Fig 1 - Creation of the mainshock-aftershock sequence



Table 2 - Mainshock-aftershock sequences

No.	Name	Country	Mainshock			Largest aftershock			Database
			Year	M _w	PGA (g)	Delay	M _w	PGA (g)	
1	Cephalonia	Greece	1983	7.0	0.18	4 hours	5.2	0.17	ITSAK
2	Alkyonides	Greece	1981	6.7	0.23	6 hours	6.4	0.12	ITSAK
3	Strofades	Greece	1997	6.6	0.15	7 minutes	6.0	0.09	ITSAK
4	Kozani	Greece	1995	6.6	0.22	3 hours	4.9	0.13	ITSAK
5	Vasiliki	Greece	1994	5.4	0.06	8 months	5.3	0.09	ITSAK
6	Vasiliki	Greece	1991	5.3	0.06	6 months	5.6	0.03	ITSAK
7	Arnaia	Greece	1995	5.3	0.04	9 days	6.6	0.04	ITSAK
8	Kalamata	Greece	1986	6.0	0.22	2 days	5.3	0.33	ITSAK
9	Athens	Greece	1999	5.9	0.11	3 minutes	4.5	0.03	ITSAK
10	Athens	Greece	1999	5.9	0.11	27 days	4.0	0.02	ITSAK
11	Volvi	Greece	1978	5.8	0.04	28 days	6.5	0.15	ITSAK
12	Ag. Paraskevi	Greece	1999	5.9	0.04	3 minutes	4.3	0.01	ITSAK
13	Athens	Greece	1999	5.9	0.26	20 minutes	4.5	0.05	ITSAK
14	Athens	Greece	1999	4.7	0.01	23 minutes	4.2	0.01	ITSAK
15	Aegion	Greece	1995	6.4	0.49	15 minutes	5.6	0.05	ITSAK
16	Friuly	Italy	1976	6.5	0.35	4 months	5.9	0.26	ESD
17	Belgrade	Yugoslavia	1979	6.9	0.45	8 hours	6.2	0.18	ESD
18	Jiashi	China	1997	6.1	0.27	2 months	5.8	0.30	USGS
19	Duzce (EW)	Turkey	1999	5.7	0.62	2 months	7.2	0.52	GDDA
20	Duzce (NS)	Turkey	1999	5.7	0.35	2 months	7.2	0.42	GDDA
21	Whittier Narrows (EW)	USA	1987	5.9	0.64	3 months	5.3	0.37	USGS
22	Whittier Narrows (NS)	USA	1987	5.9	0.45	3 months	5.3	0.26	USGS
23	Northridge (EW)	USA	1994	6.7	1.58	2 months	5.3	0.65	USGS
24	Northridge (NS)	USA	1994	6.7	1.28	2 months	5.3	0.43	USGS
25	Mammoth Lakes (EW)	USA	1980	6.1	0.42	2 days	5.9	0.40	USGS
26	Mammoth Lakes (NS)	USA	1980	6.1	0.44	2 days	5.9	0.92	USGS
27	Coalinga (EW)	USA	1983	6.4	0.58	2 months	5.8	0.84	USGS
28	Coalinga (NS)	USA	1983	6.4	0.67	2 months	5.8	1.08	USGS
29	Chi Chi (EW)	Taiwan	1999	6.2	0.97	3 hours	6.3	0.95	USGS
30	Chi Chi (NS)	Taiwan	1999	6.2	0.90	3 hours	6.3	0.40	USGS
31	Imperial Valley (EW)	USA	1979	6.5	0.59	3 minutes	5.0	0.19	USGS
32	Imperial Valley (NS)	USA	1979	6.5	0.77	3 minutes	5.0	0.37	USGS
33	Managua (EW)	Nicaragua	1972	6.2	0.42	1 hour	5.2	0.27	USGS
34	Managua (NS)	Nicaragua	1972	6.2	0.34	1 hour	5.2	0.34	USGS
35	Umbria Marche (EW)	Italy	1997	6.0	0.46	1 month	5.6	0.41	ESD
36	Umbria Marche (NS)	Italy	1997	6.0	0.52	1 month	5.6	0.38	ESD



37	Holt (EW)	Iceland	2000	6.5	0.51	4 days	6.4	0.72	ESD
38	Holt (NS)	Iceland	2000	6.5	0.63	4 days	6.4	0.42	ESD
39	Christchurch	New Zealand	2011	6.3	1.46	4 months	6.0	0.66	GEONET
40	Ancona	Italy	1972	4.5	0.53	3 hours	4.2	0.21	ESD
41	Izmit	Turkey	1999	7.6	0.36	3 months	5.8	0.80	ESD
42	Thjorsarbru (EW)	Iceland	2000	5.7	0.52	4 days	4.4	0.84	ESD
43	Thjorsarbru (NS)	Iceland	2000	5.7	0.36	4 days	4.4	0.74	ESD
44	Chokubetsu (EW)	Japan	1999	6.4	0.43	3 months	5.4	0.59	NIED
45	Chokubetsu (NS)	Japan	1999	6.4	0.40	3 months	5.4	0.28	NIED
46	Hino (EW)	Japan	2000	7.3	0.77	5 months	6.4	0.50	NIED
47	Hino (NS)	Japan	2000	7.3	0.94	5 months	6.4	0.47	NIED
48	Niimi (EW)	Japan	2000	7.3	0.84	5 months	5.9	0.83	NIED
49	Niimi (NS)	Japan	2000	7.3	0.54	5 months	5.9	0.40	NIED
50	Miyagi oki (EW)	Japan	2003	7.0	1.13	4 months	8.0	0.99	NIED
51	Miyagi oki (NS)	Japan	2003	7.0	1.12	4 months	8.0	0.82	NIED
52	Hiroo (EW)	Japan	2003	8.0	0.99	1 year	6.8	1.33	NIED
53	Hiroo (NS)	Japan	2003	8.0	0.82	1 year	6.8	1.17	NIED
54	Tsurui	Japan	2004	7.1	0.58	1 month	6.1	1.14	NIED
55	Noto Hanto	Japan	2007	6.9	0.73	1 month	5.4	0.72	NIED
56	Ehime (EW)	Japan	2007	5.3	0.51	3 months	6.8	0.52	NIED
57	Ehime (NS)	Japan	2007	5.3	0.24	3 months	6.8	0.68	NIED
58	Ichinoseki (EW)	Japan	2008	7.2	1.46	2 days	5.3	0.56	NIED
59	Ichinoseki (NS)	Japan	2008	7.2	1.16	2 days	5.3	0.70	NIED
60	Hitachi (EW)	Japan	2008	5.2	0.43	19 days	6.8	0.69	NIED
61	Hitachi (NS)	Japan	2008	5.2	0.39	19 days	6.8	1.02	NIED
62	Takane (EW)	Japan	2011	5.0	1.56	12 days	9.0	2.00	NIED
63	Takane (NS)	Japan	2011	5.0	0.39	12 days	9.0	0.77	NIED
64	Ibaraki (EW)	Japan	2011	7.7	0.94	1 day	6.7	0.72	NIED
65	Ibaraki (NS)	Japan	2011	7.7	0.57	1 day	6.7	0.54	NIED
66	Fujinomiya (EW)	Japan	2011	6.4	1.00	4 days	6.1	0.53	NIED
67	Fujinomiya (NS)	Japan	2011	6.4	0.51	4 days	6.1	1.04	NIED
68	Oshika (EW)	Japan	2011	7.1	1.35	4 days	7.0	0.63	NIED
69	Oshika (NS)	Japan	2011	7.1	1.38	4 days	7.0	0.67	NIED
70	Kitaibaraki (EW)	Japan	2011	6.4	0.51	3 months	5.5	1.08	NIED
71	Kitaibaraki (NS)	Japan	2011	6.4	0.71	3 months	5.5	0.77	NIED
72	Tsurui (EW)	Japan	2013	6.5	0.55	23 days	6.3	0.85	NIED
73	Tsurui (NS)	Japan	2013	6.5	0.71	23 days	6.3	1.25	NIED
74	Kuriyama (EW)	Japan	2013	6.3	0.85	2 months	6.0	0.58	NIED
75	Kuriyama (NS)	Japan	2013	6.3	1.25	2 months	6.0	0.30	NIED



4. Damage Indices

Damage indicators are the appropriate tools to describe the structural state with a single value. In this respect, they are used to assess the postseismic condition of a structure. For the present analysis, three overall structural damage indices (OSDIs) have been chosen due to the high interdependency level to the aforementioned seismic parameters viz. the modified overall damage index of Park and Ang ($DI_{G,P/A}$); the maximum inter-story drift ratio (MISDR); and the maximum softening index of DiPasquale and Çakmak ($DI_{D/Ç}$).

According to Park and Ang definitions [34], the local damage index is composed of two parts, namely the scaled values of the ductility and the dissipated energy of the structural element during the seismic excitation. Likewise, the global damage index, is a weighted average of the local damage at the ends of each element, with the dissipated energy as the weighting function. Thus, the local damage index ($DI_{L,P/A}$) is calculated using the following equation:

$$DI_{L,P/A} = \frac{\theta_m - \theta_r}{\theta_u - \theta_r} + \frac{\beta}{M_y \theta_u} E_T \quad (1)$$

where, θ_m the maximum rotation attained during the loading history, θ_u the ultimate rotation capacity of the section, θ_r the recoverable rotation at unloading, β a strength degrading parameter, M_y the yield moment of the section and E_T the dissipated hysteretic energy. The Park and Ang damage index is a linear combination of the maximum ductility and the hysteretic energy dissipation demand imposed by the earthquake on the structure. In this study, the numerical value of parameter β in Eq. (1) is equal to 0.1. The value corresponds to nominal strength degradation.

The overall (global) value for the Park and Ang index is derived from the following equation:

$$DI_{G,P/A} = \frac{\sum_{i=1}^n DI_{L,P/A} E_i}{\sum_{i=1}^n E_i} \quad (2)$$

where E_i is the energy dissipated the location i and n is the number of positions at which local damage is computed. Although the $DI_{G,P/A}$ value may exceed unity, the structural failure is assumed to occur when the value of $DI_{G,P/A}$ ranges from 0.80 to 1.00. Under elastic response the value of $DI_{G,P/A}$ should theoretically be zero; however, according to experimental data the values of $DI_{G,P/A}$ in the elastic range are not explicitly equal to zero but present a minor upward trend.

The maximum inter-story drift ratio (MISDR) has been selected as a second OSDI [35]. It is defined as the maximum story drift (u_{max}) normalized by the story height (h), as given by the relation:

$$MISDR = \frac{|u|_{max}}{h} 100[\%] \quad (3)$$

The maximum softening index of DiPasquale and Çakmak ($DI_{D/Ç}$) is based on the dynamic characteristics of structures [36]. It is given by the expression:

$$DI_{D/Ç} = 1 - \frac{T_0}{T_{max}} \quad (4)$$

where T_0 is the fundamental period of the examined structure acquired by dynamic analysis and T_{max} is the maximum natural period of the examined structure during the seismic excitation. For the evaluation of T_{max} , the instantaneous natural period is required to be evaluated, which is accompanied by the actual time-dependent tangent stiffness matrix. The natural period computed for each time step of a nonlinear dynamic analysis shows high variability. Since the duration of the maxima is very short, their influence in the natural period of an equivalent linear system is not significant. Thus, a more meaningful indication of the change in the natural period can be obtained by observing a moving average of the instantaneous natural period using a sliding time window for the smoothness of the time versus fundamental period curve. The time-fundamental period curve can be evaluated by a nonlinear dynamic procedure that calculates the fundamental period of the structure by considering the stiffness degradation in every time step [37].



5. Application

The symmetric reinforced concrete frame structure is shown in Fig. 2, has been designed according to the European standards Eurocodes 2 and 8 (EC2 and EC8) [38, 39]. The structure has been classified as Structural Class 4 (S4), ductility class M and belongs to Seismic Zone II (PGA=0.24g). The column cross section decreases by 5 cm after the second, fourth and sixth story respectively as the load bearing demand lessens. The cross sections of the beams are considered as T-beams with 30 cm width, 20 cm slab thickness, 60 cm total beam height, 1.80 m effective width for the "T" type beams and 1.15 m effective width for the "L" type beams. The distances between each frame of the structure are equal to 6 m while the ground floor has a 4 m height and all subsequent floors 3 m. The subsoil was of type C (deep deposits of medium dense sand or stiff clay at least 50 m thick). The fundamental period of the selected frame were 1.30 s.

In a follow-up of the design procedure, a nonlinear dynamic analysis is used to evaluate the seismic structural response, exploiting the set of natural mainshock and mainshock-aftershock sequences previously described and the aid of the computer program IDARC 2D. A three-parameter Park model specifies the hysteretic behavior of beams and columns at both ends of each member. This hysteretic model incorporates stiffness degradation, strength deterioration, slip-lock and a tri-linear monotonic envelope. Experimental results of cyclic force-deformation characteristics of typical components of the studied structure specify the parameter values of the above degrading parameters. This study uses the nominal parameter for stiffness degradation. While the seismic excitation time step differs for each event, the selected time step for the structural analysis is set at 0.01 s. Among the several response parameters, the focus is on the overall structural damage indices (OSDIs) described in the previous section.

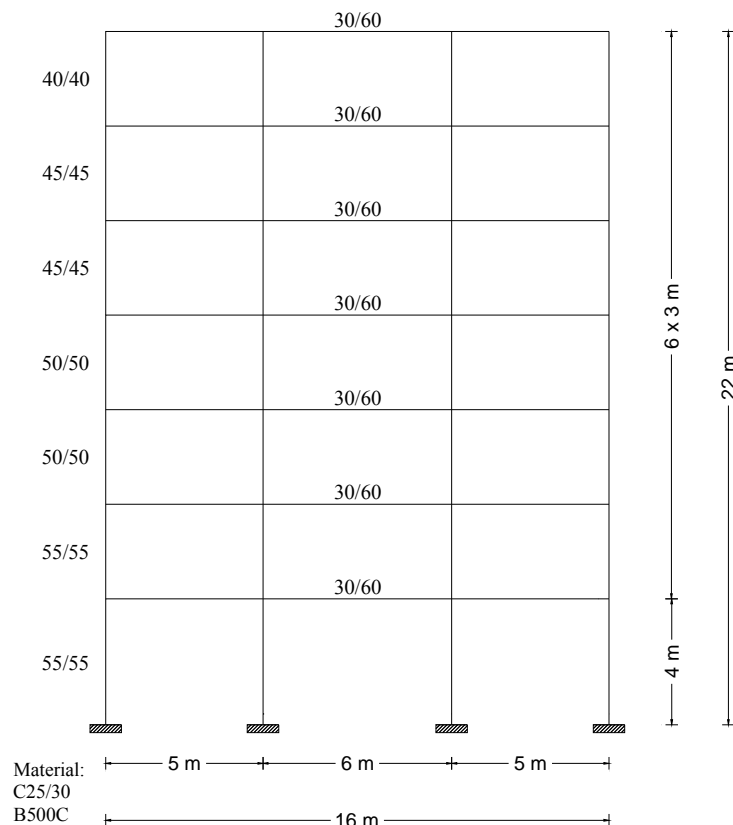


Fig 2 – Reinforced concrete frame structure



6. Statistical Analysis

The interdependency level between the selected seismic parameters and damage indices is calculated with the use of correlation coefficients. A correlation coefficient is a coefficient that illustrates a quantitative measure that describes the statistical relationship between two observed data values. In the present work, the chosen correlation coefficients are the Pearson correlation and the Spearman's rank correlation coefficient [40, 41].

The Pearson correlation coefficient is used to measure the strength of a linear association between two variables, where the value $r = 1$ means a linear positive correlation and the value $r = -1$ means a linear negative correlation and is given by the relation:

$$r_{\text{Pearson}} = \frac{\sum_{i=1}^N (X_i - \bar{X})(Y_i - \bar{Y})}{\sqrt{\sum_{i=1}^N (X_i - \bar{X})^2 \sum_{i=1}^N (Y_i - \bar{Y})^2}} \quad (5)$$

where: \bar{X} and \bar{Y} are the mean values of X_i and Y_i data respectively and N is the number of pairs of values (X_i, Y_i) in the data.

The Spearman rank correlation coefficient between two variables X and Y , is given by the relation:

$$r_{\text{Spearman}} = 1 - \frac{6 \sum_{i=1}^N D^2}{N(N^2 - 1)} \quad (6)$$

where D denotes the differences between the ranks of corresponding values of X_i and Y_i , moreover, N is the number of pairs of values (X, Y) in the data.

Table 3 presents the correlation coefficients between the seismic parameters and the selected damage indices.

Table 3 – Correlation coefficients between the seismic parameters and the OSDIs.

Seismic Parameters	Pearson correlation			Spearman rank correlation		
	DI _{G,P/A}	MISDR	DI _{D/C}	DI _{G,P/A}	MISDR	DI _{D/C}
PGA	0.374	0.334	0.640	0.618	0.607	0.605
PGV	0.437	0.424	0.314	0.601	0.609	0.615
PGD	0.409	0.403	0.313	0.542	0.552	0.564
PGA/PGV	0.373	0.364	0.522	0.456	0.472	0.477
CP	0.643	0.678	0.292	0.408	0.389	0.392
1/CP	0.424	0.400	0.353	0.408	0.389	0.392
SI _H	0.884	0.830	0.767	0.971	0.962	0.961
SI _K	0.810	0.750	0.696	0.926	0.912	0.920
SI _{MR}	0.383	0.344	0.640	0.625	0.614	0.611
SI _{H/C}	0.631	0.557	0.733	0.896	0.891	0.886
SI _{N/H}	0.814	0.738	0.760	0.959	0.947	0.947
T _M	0.167	0.161	0.266	0.168	0.168	0.199
EPA	0.344	0.310	0.686	0.660	0.664	0.652
EPA _{max}	0.419	0.376	0.697	0.671	0.671	0.661
CAV	0.350	0.342	0.511	0.668	0.669	0.688
CAD	0.410	0.403	0.315	0.584	0.590	0.610
CAX	0.346	0.339	0.510	0.667	0.669	0.688
SD	0.834	0.775	0.710	0.934	0.920	0.925
SV	0.778	0.706	0.737	0.922	0.910	0.904
SA	0.486	0.418	0.711	0.706	0.691	0.692
SMD _{T/B}	0.192	0.165	0.435	0.369	0.386	0.411
SMD _{B0.05}	0.327	0.326	0.587	0.480	0.495	0.509



SMD _{B0.10}	0.318	0.302	0.620	0.516	0.532	0.547
SMD _{Don}	0.272	0.263	0.434	0.393	0.408	0.432
SMD _{T/N}	0.231	0.223	0.265	0.300	0.311	0.357
SMD _{McCann}	0.263	0.211	0.326	0.346	0.337	0.385
P _{0.90}	0.297	0.274	0.411	0.668	0.664	0.656
P _{B0.05}	0.378	0.341	0.549	0.672	0.667	0.665
P _{B0.10}	0.340	0.310	0.503	0.581	0.573	0.567
P _{Don}	0.214	0.193	0.367	0.649	0.646	0.639
P _{T/N}	0.302	0.265	0.532	0.631	0.625	0.606
P _{McCann}	0.222	0.199	0.291	0.302	0.308	0.274
I _{F/V/F}	0.399	0.378	0.302	0.595	0.604	0.612
E _{inp}	0.440	0.447	0.294	0.621	0.623	0.642
SI _M	0.379	0.340	0.640	0.620	0.609	0.607
SI _{Mmod}	0.383	0.344	0.641	0.624	0.613	0.610
DP _{A/S}	0.763	0.826	0.364	0.816	0.807	0.820
I _o	0.297	0.296	0.453	0.691	0.690	0.698
RMS _a	0.432	0.385	0.682	0.662	0.658	0.661

7. Conclusion

In this paper, 75 artificial seismic recordings, created by the joining of two natural accelerograms that represent the mainshock-aftershock sequence were utilized to examine the effect of seismic sequence in the interrelationship between several seismic parameters and the chosen damage indices. The examined structure is a seven-story reinforced concrete frame structure designed under the European design standards for reinforced concrete and antiseismic structures (EC2, EC8). After subjecting the structure in a nonlinear dynamic analysis for all the seismic excitations, the damage indices values were furnished. These indices are the OSDI after Park and Ang, the MISDR, and the global damage index after DiPasquale and Çakmak. The next step was the correlation study between the seismic parameters and the damage indices. The correlation methods used are the Pearson correlation coefficient and the Spearman rank correlation. The correlation study between the damage indices and the seismic parameters has produced the following results:

- The results show poor Pearson and Spearman correlation between the SMD_{T/B}, SMD_{B0.05}, SMD_{B0.10}, SMD_{Don}, SMD_{T/N}, SMD_{McCann} and the examined damage indices.
- The Meskouris earthquake type T_M shows the lowest correlation level with the damage indices.
- High correlation levels are observed between SI_H, SI_K, SI_{H/C}, SI_{N/H}, SD, SV, DP_{A/S} and the examined damages indices.
- The Spearman rank correlation produces a slightly higher interdependency level than the Pearson correlation between the seismic parameters and the selected damage indices.
- Concluding, the spectral seismic parameters are reliable descriptors of the seismic sequence damage potential and can be used to assess the postseismic status of a structure reliably.

8. Acknowledgements

The authors gratefully acknowledge the financial support given by ETAA.

9. References

- [1] Omori F (1895): On the aftershocks of earthquakes. *Journal of Colloid Science*, **7** (2), 111-200.
- [2] Mahin SA (1980): Effects of duration and aftershocks on inelastic design earthquakes. *Proceedings of the seventh world conference on earthquake engineering*, **5**, 677-680.



- [3] Zhai C-H, Wen W-P, Li S, Chen Z, Chang Z, Xie L-L (2014): The damage investigation of inelastic SDOF structure under the mainshock–aftershock sequence-type ground motions. *Soil Dynamics and Earthquake Engineering*, **59**, 30-41.
- [4] Ruiz-García J, Moreno J, Maldonado I (2008): Evaluation of existing Mexican high-way bridges under mainshock–aftershock seismic sequences. In: *Proceedings of the 14th world conference on earthquake engineering*. Paper 05-02-0090.
- [5] Hatzigeorgiou G, Liolios A (2010): Nonlinear behaviour of RC frames under repeated strong ground motions. *Soil Dynamics and Earthquake Engineering*, **30**, 1010-25.
- [6] Ruiz-García J, Negrete-Manriquez J (2011): Evaluation of drift demands in existing steel frames under as-recorded far-field and near-fault mainshock–aftershock seismic sequences. *Engineering Structures*, **33**, 621-634.
- [7] Zhang S, Wang G, Sa W (2013): Damage evaluation of concrete gravity dams under mainshock–aftershock seismic sequences. *Soil Dynamics and Earthquake Engineering*, **50**, 16-27.
- [8] Cabañas L, Benito B, Herráiz M (1997): An approach to the measurement of the potential structural damage of earthquake ground motions. *Earthquake Engineering and Structural Dynamics*, **26** (1), 79-92.
- [9] Elenas A, Meskouris K (2001): Correlation study between seismic acceleration parameters and damage indices of structures. *Engineering Structures*, **23** (6), 698-704.
- [10] Elenas A (2000): Correlation between seismic acceleration parameters and overall damage indices of buildings. *Soil Dynamics and Earthquake Engineering*, **20** (1), 93-100.
- [11] Elenas A (2011): Intensity parameters as damage potential descriptors of earthquakes. *COMPADYN 2011*, Corfu, Greece.
- [12] Reinhorn AM et al. (2009): IDARC2D version 7.0: A program for the inelastic damage analysis of structures. *Technical Report, MCEER-09-0006*, MCEER, State University of New York at Buffalo, New York, USA.
- [13] Meskouris K (2000): *Structural Dynamics: Models, Methods, Examples*. Ernst & Sohn, Berlin, Germany.
- [14] Vanmarcke EH, Lai SSP (1980): Strong-motion duration and RMS amplitude of earthquake records. *Bulletin of the Seismological Society of America*, **70** (4), 1293-1307.
- [15] Housner GW (1952): Spectrum intensities of strong motion earthquakes. *Proceedings of the Symposium on Earthquake and Blast Effects on Structures*, EERI, Oakland, California, USA, 20-36.
- [16] Kappos AJ (1990): Sensitivity of calculated inelastic seismic response to input motion characteristics. *Proceedings of the 4th U.S. National Conference on Earthquake Engineering*, EERI, Oakland, California, USA, 25-34.
- [17] Martinez-Rueda JE (1998): Scaling procedure for natural accelerograms based on a system of spectrum intensity scales. *Earthquake Spectra*, **14** (1), 135-152.
- [18] Hidalgo P, Clough RW (1974): Earthquake Simulator Study of a Reinforced Concrete Frame. *Report UCB/EERC-74/13*, EERC, University of California, Berkeley, USA.
- [19] Nau M, Hall WJ (1984): Scaling Methods for Earthquake Response Spectra. *Journal of Structural Engineering*, **110** (7), 1533-1548.
- [20] Meskouris K, Krätzig WB, Hanskötter U (1993): Nonlinear computer simulations of seismically excited wall-stiffened reinforced concrete buildings. *Proceedings of the 2nd International Conference on Structural Dynamics (EURODYN '93)*, Balkema, Lisse, the Netherlands, 49-54.
- [21] Tentative Provisions for the Development of Seismic Regulations for Buildings (1978): ATC 3-06 Publication, US Government Printing Office, Washington, DC, USA.



- [22] Chopra AK (1995): *Dynamics of Structures*. Prentice-Hall, Englewood Cliffs, NJ, USA.
- [23] Trifunac MD, Brady AG (1975): A study on the duration of strong earthquake ground motion. *Bulletin of the Seismological Society of America*, **65** (3), 581-626.
- [24] Page RA, Boore DM, Joyner WB, Coulter HW (1972): Ground Motion Values for Use in Seismic Design of Trans-Alaska Pipeline System. *USGS Circular 672*, U.S. Geological Survey, Washington, DC, USA.
- [25] Donovan NC (1972): Earthquake hazard for buildings. *Building Science Series* **46**, 82-111.
- [26] Novikova EI, Trifunac MD (1993): Duration of Strong Earthquake Ground Motion. Physical Basis and Empirical Equations. *Report No. 93-02*, Department of Civil Engineering, University of Southern California.
- [27] McCann MW, Shah HC (1979): Determining strong-motion duration of earthquakes. *Bulletin of the Seismological Society of America*, **69**, 1253-1265.
- [28] Jennings PC (1982): *Engineering seismology, in Earthquakes: Observation, Theory and Interpretation*. Italian Physical Society, Varenna, Italy, 138-173.
- [29] Fajfar P, Vidic T, Fischinger M (1990): A measure of earthquake motion capacity to damage medium-period structures. *Soil Dynamics and Earthquake Engineering*, **9** (5), 236-242.
- [30] Uang C-M, Bertero VV (1990): Evaluation of seismic energy in structures. *Earthquake Engineering & Structural Dynamics*, **19** (1), 77-90.
- [31] Matsumura K (1992): On the intensity measure of strong motions related to structural failures. *Proceeding of 10 WCEE*, **1**, 375-380.
- [32] Araya R, Saragoni GR (1984): Earthquake accelerogram destructiveness potential factor. *Proceedings of the 8th World Conference on Earthquake Engineering*, EERI, El Cerrito, California, USA, 835-842.
- [33] Arias A (1970): A Measure of Earthquake Intensity. *Seismic Design for Nuclear Power Plants*, MIT Press, Cambridge Massachusetts, 438-483.
- [34] Park YJ, Ang AH-S (1985): Mechanistic seismic damage model for reinforced concrete. *Journal of Structural Engineering*, **111** (4), 722-739.
- [35] Structural Engineers Association of California (SEAOC) (1995): Vision 2000: Performance based seismic engineering of buildings. Sacramento, California.
- [36] Di Pasquale E, Çakmak A (1987): Detection and assessment of seismic structural damage. *Technical report NCEER-87-0015*, State University of New York, Buffalo.
- [37] Elenas A (2014): Seismic-Parameter-Based Statistical Procedures for the Approximate Assessment of Structural Damage. *Mathematical Problems in Engineering*, Article ID 916820, 22.
- [38] EC2, Eurocode 2 (2000): *Design of Concrete Structures*. Part 1: General Rules and Rules for Buildings, European Committee for Standardization, Brussels, Belgium.
- [39] EC8, Eurocode 8 (2004): *Design of Structures for Earthquake Resistance*. Part 1: General Rules, Seismic Actions, and Rules for Buildings, European Committee for Standardization, Brussels, Belgium.
- [40] Montgomery DC, Runger GC (2003): *Applied Statistics and Probability for Engineers*. John Wiley & Sons, New York, NY, USA.
- [41] Navidi W (2011): *Statistics for Engineers and Scientists*. McGraw-Hill, New York, NY, USA.